21st Australasian Fluid Mechanics Conference
Adelaide, Australia
10-13 December 2018

The effect of aspect ratio on the flow characteristics of a Hybrid Solar Receiver Combustor

S. Long[1], T.C.W. Lau[1], A. Chinnici[1], Z.F. Tian[1], B.B. Dally[1], G.J. Nathan[1]

[1] Centre for Energy Technology, School of Mechanical Engineering
The University of Adelaide, Adelaide, South Australia 5005, Australia.

Abstract

We present a systematic experimental study of the interaction between four rotationally-symmetric jets within a cylindrical chamber, under conditions relevant to a wide range of practical applications, including the Hybrid Solar Receiver Combustor (HSRC). The HSRC geometry is simplified here to a cylindrical cavity with four inlet jets (representing four burners), which are configured in an annular arrangement and aligned at an inclination angle (α_j) to the axis with a tangential component (azimuthal angle θ_j) to generate a swirl in the chamber. In this study, we assess the configurations of $\alpha_j = 25^\circ$ and $\theta_j = 5^\circ$. The length of the chamber was varied from L_c = 148 mm to 74 mm and the diameter of the chamber was D_c = 74 mm, resulting in an aspect ratio of L_c/D_c = 2, 1.5 and 1. The inlet Reynolds number for each injected jet and the number of jets were fixed at Re_D = 10,500 and 4, respectively. Velocity data obtained with Particle Image Velocimetry (PIV) were used to characterise the large-scale flow field within the selected experimental configurations. The results reveal a significant dependence of the mean flow-field on the aspect ratio L_c/D_c for the value of α_j and θ_j considered here. More specifically, it was found that L_c/D_c can influence the position of the external recirculation zone (ERZ), the strength of the central resulting jet, and the recirculation rate (K_v).

Introduction

Multiple jets have been widely used in many practical applications as solar receiver reactors [9], gas turbine engines [5], longitudinal ventilation systems [3] and separated-jet combustors [1]. However, the greater complexity of these configurations over the single round jet issuing into a quiescent environment [8], including the additional parameters and experimental challenges, means many gaps in understanding remain. Of particular interest here are the configurations featuring multiple-jets relevant to the Hybrid Solar Receiver Combustor (HSRC) under development at the University of Adelaide [3,4,10,11,12,13]. The HSRC offers potential to reduce both the energy losses and total infrastructure requirements relative to a hybrid from stand-alone components, while providing a firm supply of energy for heat and power applications. The geometry of a typical HSRC (Figure 1) features a cavity that is operable as either a cavity receiver or a combustion chamber equipped multiple burners to direct fuel and air into the main cavity, and tubular heat exchangers to transfer the thermal energy to the heat transfer fluid. The burners are configured in an annular ring arrangement and aligned at an inclination angle (α_j) relative to the axis of the cavity, and/or at an azimuthal angle (θ_j) to the axis of the burner, resulting in a swirling flow within the main cavity. This burner arrangement, referring to the conditions where both $\alpha_j > 0^\circ$ and $\theta_j > 0^\circ$, is termed "rotationally-symmetric". Previous investigations of the flow-fields within the HSRC revealed a significant dependence of the jet angles (α_j and θ_j) on the strength and position of the large-scale recirculation which is critical for achieving flow conditions conducive for efficient receiver operation [11,12]. Nevertheless, the dependence of the geometrical parameters, such as the length (L_c) and diameter (D_c) of the chamber, on important flow characteristics remains unknown, although relevant studies have found that the aspect ratio of L_c/D_c is critical for maintaining high thermal efficiency with low infrastructure costs [10, 13]. Hence, a comprehensive understanding of the effect of aspect ratio L_c/D_c is needed to characterize the flow-fields of multiple jets.

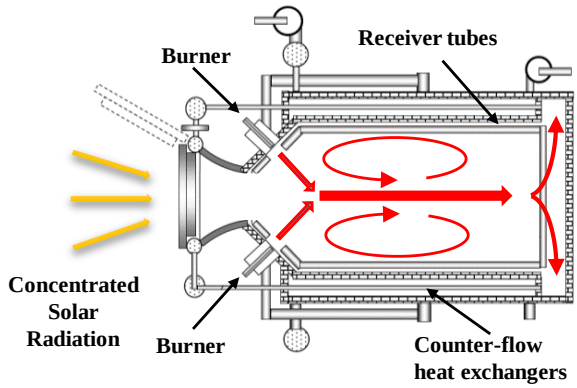

Figure 1. Hybrid Solar Receiver Combustor

Previous studies of flow-fields generated with multiple symmetric jets within a confined space revealed that the flow structure depends strongly on the arrangement and geometric features of jets [1,2,6,11,15,16,17]. However, to our knowledge, little or no information is available for the key geometrical parameters (e.g., L_c and D_c) of the confined space for multiple jets configurations. In addition, our previous work Long et al [12] revealed the presence of an external recirculation zone (ERZ) within a cylindrical chamber. The ERZ is typically associated with the recirculation rate (K_v) within the chamber, which is particularly critical for combustion stabilization and thermal efficiency [18]. However, the influence of L_c/D_c on the recirculation regions is not fully understood.

In light of the needs above, the present paper reports on an experimental investigation of the iso-thermal flow-fields generated with a Multiple Impinging Jets in a Cylindrical Chamber, termed "MIJCC". The aims of the current study are: (a) to identify the influence of the aspect ratio L_c/D_c on the mean flow-fields within a cylindrical chamber with multiple-jets; and (b) to characterize the dependence of the characteristics of large-scale recirculation zones on the aspect ratio L_c/D_c.

Methodology

A schematic diagram of the experimental MIJCC configuration is shown in Figure 2. The cavity of the experimental model consists of a cylindrical chamber with a conical expansion, connected with a secondary concentrator (SC). The geometric parameters are given in Table 1.

The length of the MIJCC chamber were L_c = 148 mm, 111 mm and 74 mm, resulting in an aspect ratio of L_c/D_c = 2, 1.5 and 1. In addition, the chamber length of our previous work L_r = 225 mm, resulting in L_r/D_c = 3, was chosen as reference cases for

comparison with the present study (labelled with an asterisk in Table 2).

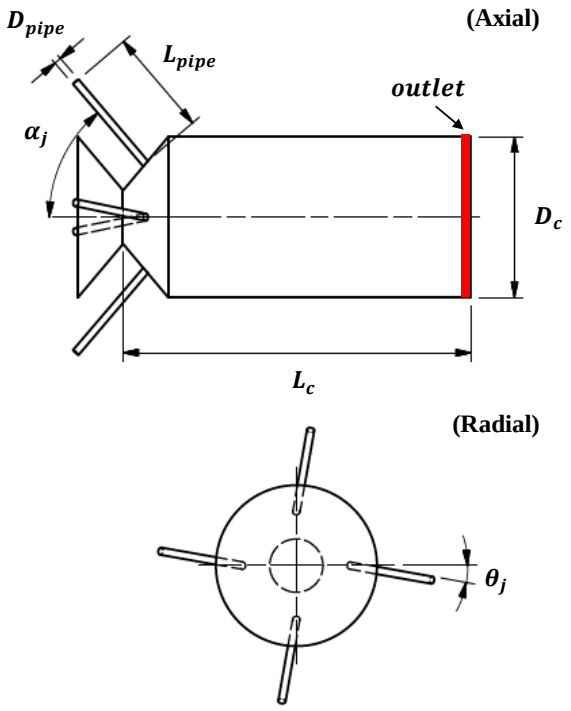

Figure 2. Schematic diagram of the configuration of the Multiple Impinging Jets in a Cylindrical Chamber (MIJCC).

Dimensions	Description	Value
D_c	Chamber diameter	74 mm
L_c	Chamber length	148, 111, 74 mm
L_r	Reference chamber length	225 mm
L_{pipe}	Inlet pipe length	150 mm
D_{pipe}	Inlet pipe diameter	3.35 mm
α_j	Jet inclination angle	25°
θ_j	Jet azimuthal angle	5°

Table 1. Values of the key geometric parameters of the experimental models.

Experimental case No.	Configurations	Confinement aspect ratio, L_c/D_c
1	MIJCC-05-LD20	2
2	MIJCC-05-LD15	1.5
3	MIJCC-05-LD10	1
4*	MIJCC-05-LD30	3

Table 2. The notation for the configurations investigated experimentally in the present study.

Particle Image Velocimetry (PIV) was employed under isothermal conditions at ambient temperature, with water as the working fluid to avoid deposition of tracer particles onto confining walls. The entire device was fully submerged into a rectangular water tank to minimize optical distortion. The water from the outlets was discharged into the water tank, which overflowed to a reservoir. The discharged fluid was reinjected through the jets using a water pump, a frequency converter and flowmeters, resulting in a closed-loop system.

The inlet jet bulk injection velocity at the nozzle exit (U_e) was fixed at 2.8 m/s for each nozzle, leading to an inlet jet Reynolds number Re_D = 10,500. This ensures that the inlet flow is within the fully turbulent regime. The inclined jets were introduced through long straight pipes with a length-to-diameter ratio, L_{pipe}/D_{pipe} = 46, which is sufficient to closely approach a fully-developed inflow condition at the exit of the inlet nozzles [14] and thus generate a well-defined inflow condition to the chamber.

The flow was seeded with hollow glass spheres of 12 μm in diameter and with a specific gravity of 1.1. The resultant Stokes number (Sk_D) was estimated to be Sk_D = 0.003 (where ρ_p is the particle density). This is sufficiently low to enable the particles to follow the flow down to length scales that can be resolved with the PIV measurement.

The optical arrangement and the measurement region are shown schematically in Figure 3. The source of illumination for the PIV measurements was a double-head, pulsed Nd:YAG laser (Quantel Brilliant B), operating at a fixed pulsing frequency of 10 Hz and a maximum power of approximately 400 mJ. The laser was operated in the frequency-doubled mode to provide a wavelength of 532 nm. The thickness of the light sheet was estimated to be 1.5 mm at the focal line.

The images were captured with a Charged Coupled Device (CCD) camera with an array of 1920 × 1080 pixels, which provides the axial (u) and radial (v) instantaneous velocity components with an image size of 118 mm (L_i) × 66 mm (W_i). A minimum of 3000 PIV images (12 bits) was recorded for each measurement. The image-processing was performed with an in-house PIV code in MATLAB, with an interrogation window size of 32 × 32 pixels, leading to a spatial resolution of 2 mm in each direction. A multi-grid correlation algorithm with 50% overlap was applied to all cases. All erroneous vectors were removed from the ensemble. The overall uncertainty of the mean velocity field was calculated to be 5%.

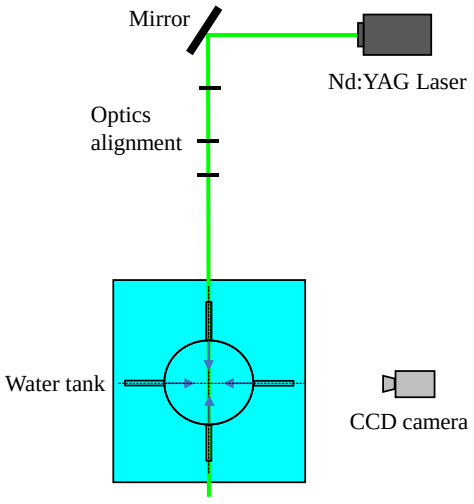

Figure 3. Experimental layout for the PIV measurements, together with the optical arrangement.

Results and discussion

Figure 4 presents the contours of measured mean axial velocity (U_x) normalized by the nozzle exit velocity (U_e), showing the streamlines, labelled with arrows to indicate flow direction (white arrows), and magnitude (colour map) for the configuration of α_j = 25° and θ_j = 5° with (a) L_c/D_c = 2, (b) L_c/D_c = 1.5, and (c) L_c/D_c = 1. The dashed line (in white colour) denotes the upstream end of the exit plane. It can be seen that a

central resulting jet flow (enclosed with red dashed box) occurs in all cases downstream from a merging point of the four inlet jets. This resulting jet generates an external recirculation zone (ERZ), whose vortex core is marked with a black "×", running almost the full length of the chamber. It can also be seen that the position of the ERZ depends strongly on the value of L_c/D_c. For example, the axial location of the ERZ vortex-core relative to the throat location, x_{core}, increases from $x_{core}/L_c = 0.36$ to 0.40 and then reduces to $x_{core}/L_c = 0.27$ as L_c/D_c is reduced from 2 to 1 [Fig. 4(a), (b) and (c), respectively], with the distance between the ERZ vortex-core and the bluff end-wall reduces to $x_{end}/L_c \approx 0.09$ at $L_c/D_c = 1.5$ and remains approximately the same for $L_c/D_c = 1$. In addition, this decrease in L_c/D_c also increases the radial location of the ERZ core from $r_{core}/D_c = 0.28$ at $L_c/D_c = 2$ to $r_{core}/D_c = 0.4$ at $L_c/D_c = 1$. These findings are attributed to the effect of jet impingement on the bluff end-wall that influences the development of the resulting jet flow, and is consistent with previous studies with an unconfined single jet [7].

The results in Figure 4 also show that a reduction in L_c/D_c leads to ≈ 30% increase in the velocity magnitude of the jets upstream from the merging point (above the red dashed-box). This is attributed to the reduced flow oscillation at and upstream from the merging point as L_c is decreased. That is, a shorter length of the chamber tends to restrict both the "in-plane" and "out-of-plane" motion of the four inlet-jets, which in turn inhibits the flow oscillation associated with the interaction between inlet-jets.

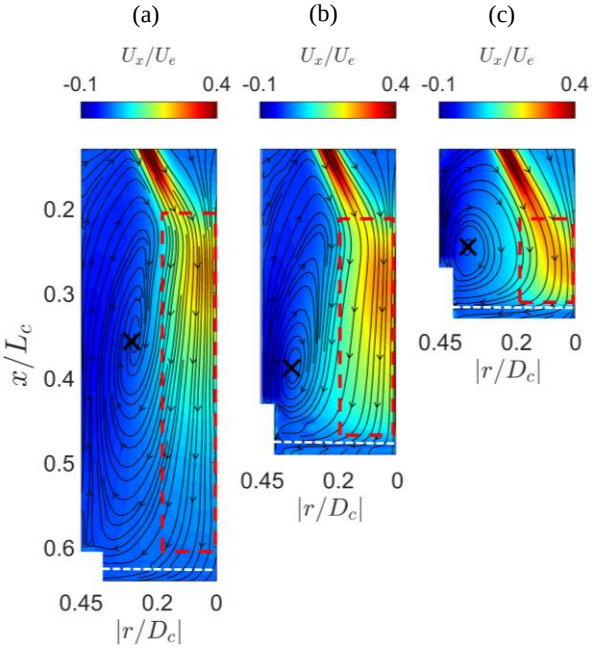

Figure 4. Mean axial velocity (U_x) normalized by the bulk mean jet exit velocity (U_e), showing the streamlines, labelled with arrows to indicate flow direction (black arrows), and magnitude (colour map), for (a) $L_c/D_c = 2$, (b) $L_c/D_c = 1.5$, and (c) $L_c/D_c = 1$.

Figure 5 presents the evolution of dimensionless mean axial velocity (U_c/U_e) along the axis of the MIJCC device for all investigated conditions. The PIV data from our previous work [12] of $L_c/D_c = 3$ is also included. The dotted lines refer to the locations of the bluff end-wall. We define the jet merging point, P_{mer}, to be the location of the maximum mean axial velocity along the centreline of the chamber [$(U_c/U_e)_{max}$]. It can be seen that $(U_c/U_e)_{max} \approx 0.25$ at $x/L_r = 0.27$ for all cases, implying that L_c/D_c does not change the location of the merging point or its corresponding velocity magnitude. However, downstream from P_{mer}, the evolution of U_c/U_e is strongly influenced by L_c/D_c. For example, as L_c/D_c reduces from 2 to 1.5, the decay rate of U_c/U_e decreases significantly. This is possibly caused by the effect of end-wall on the development of resulting jet that reduces the entrainment rate between the jet and surrounding fluids. Importantly, for $L_c/D_c = 1$ where the bluff end-wall closely approaches the location of P_{mer}, the central resulting jet is almost absent [also see Fig 4(c)] due to the confinement effect from the cylindrical walls, while the decay of U_c/U_e is the highest for all cases. Hence, it can be concluded that the aspect ratio of L_c/D_c significantly inhibits the axial development of the central resulting jet for $L_c/D_c < 2$.

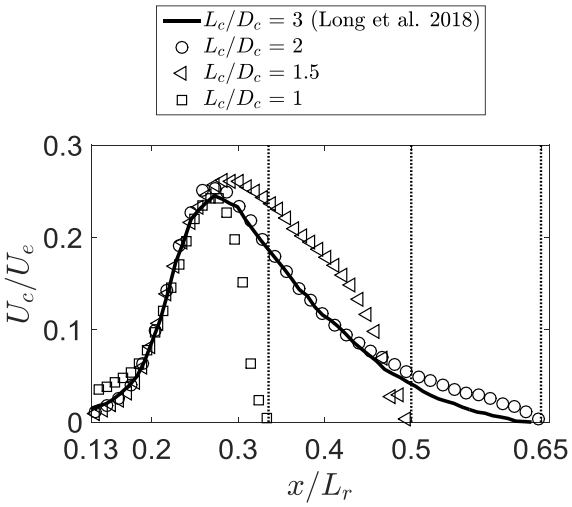

Figure 5. Evolution of mean axial velocity along the centerline of the Multiple Impinging Jets in a Cylindrical Chamber (MIJCC), normalized by the bulk mean velocity (U_c/U_e) as functions of chamber length for all experimental cases. For clarity, the figure only presents one in two data points.

Figure 6 presents the effect of L_c/D_c on the recirculation rate ($Kv = \dot{m}_{ent}/\dot{m}_{in}$) within the MIJCC configurations. Here $\dot{m}_{ent} = \int_0^\infty 2\pi r \rho U_{ent}\, dr$ is the total mass flow rate of fluid transported upstream through a plane orthogonal to the axis at the plane x/L_c, while $\dot{m}_{in}$ refers to the total inlet mass flow rate of fluid. The entrainment velocity, U_{ent}, is the negative axial velocity ($U_x < 0$) within the chamber. It can be seen that a single hump profile, approximately corresponding with the axial extent of the ERZ, occurs for all cases, while the location of the peak value of K_v [$(K_v)_{max}$] coincides well with the location of the vortex-core in the ERZ (x_{core}). For $L_c/D_c = 2$ to 1.5, a decrease in L_c/D_c leads to a decrease in the axial extent of K_v throughout the chamber ($x/L_r = 0.13$ to 0.65), although the magnitude of $(K_v)_{max}$ for these two cases remains the same (occurring at $x/L_r = 0.38$). However, as L_c/D_c is further decreased to $L_c/D_c = 1$, the value of $(K_v)_{max}$ increases significantly (~ 25%) and its location moves further upstream to $x/L_r = 0.2$ due to the confinement effect caused by the chamber length. Hence, the axial profile of K_v appears similar for $L_c/D_c \geq 2$, while as L_c is further reduced to 1, the value and distribution of K_v is strongly restricted by the chamber length and bluff end wall.

The results in Figure 6 also shows that the value of $(K_v)_{max}$ exceeds 3 for all cases considered here. This finding is important for the development of practical combustion applications, particularly those employing combustion in the MILD (moderate or intense low-oxygen dilution) regime [18]. This is because the value of $K_v = 3$, in addition to the presence of a large and uniform recirculation zone, is crucial for achieving desirable mixing, heat transfer and quasi-

homogeneous temperature distribution for applications employing MILD (such as the HSRC).

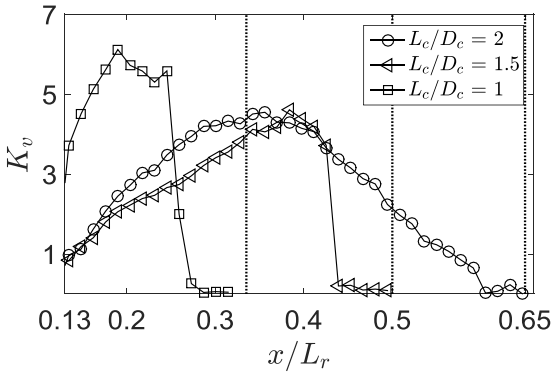

Figure 6. Evolution of the recirculation rate (K_v) along the centerline of the Multiple Impinging Jets in a Cylindrical Chamber (MIJCC) as a function of the normalized reference chamber length (x/L_r).

Conclusions

An experimental study was carried out to investigate the iso-thermal flow field within a cylindrical chamber featuring multiple-jets with an inclination angle $\alpha_j = 25^\circ$ and an azimuthal angle $\theta_j = 5^\circ$. The aspect ratio of chamber length to diameter (L_c/D_c) from 2 to 1 was assessed in the present study. The key outcomes of the study are as follows:

1. For a given value of D_c, the mean velocity field depends strongly on the value of L_c as L_c/D_c is reduced from 2 to 1. This causes a significant reduction in the axial location and the velocity magnitude of the external recirculation zone (ERZ).
2. A decrease in L_c/D_c from 2 to 1 was found to increase 30% of the velocity magnitude near to the merging point, which highlights the reduction in the large-scale oscillations as L_c/D_c is reduced.
3. The maximum value of the recirculation rate of the ERZ (K_v) was found to increase by 25% as L_c/D_c reduces from 2 to 1, with the axial extent of K_v reduces 50%.
4. The value of K_v exceeds 3 for all cases, which is crucial for achieving desirable mixing, heat transfer and quasi-homogeneous temperature for solar thermal applications utilising combustion in the MILD regime.

Acknowledgments

The authors would like to acknowledge the support of the Australian Research Council, FCT Combustion Pty. Ltd. and Vast Solar Pty. Ltd. through the ARC Linkage grant LP110200060. Mr. Shen Long acknowledges the financial support of the Australian Government Research Training Program.

References

[1] Boushaki, T. & Sautet, J.C., Characteristics of flow from an oxy-fuel burner with separated jets: influence of jet injection angle. *Exp. Fluids*, **48**, 2010, 1095-1108.

[2] Chammem, T., Mhiri, H. & Vauquelin, O., Experimental and computational investigation of Reynolds number effect on the longitudinal ventilation in large enclosure of twin inclined jets. *Build. Environ*., **67**, 2013, 87-96.

[3] Chinnici, A., Tian, Z.F., Lim, J.H., Nathan, G.J. & Bassam, B.B., Comparison of system performance in a hybrid solar receiver combustor operating with MILD and conventional combustion. Part I: Solar-only and combustion-only employing conventional combustion." *Sol. Energy*, **147**, 2017, 489-503.

[4] Chinnici, A., Tian, Z.F., Lim, J.H., Nathan, G.J. & Bassam, B.B., Comparison of system performance in a hybrid solar receiver combustor operating with MILD and conventional combustion. Part II: Effect of the combustion mode. *Sol. Energy*, **147**, 2017, 479-488.

[5] Cox, G., Multiple jet correlations for gas turbine engine combustor design. *J. Eng. Power*, **98**, 1976, 265-272.

[6] Gao, Z., Han, J., Xu, Y., Bao, Y. & Li, Z., Particle image velocimetry (PIV) investigation of flow characteristics in confined impinging jet reactors. *Ind. Eng. Chem. Res.*, **52**, 2013,11779-11786.

[7] Guo, T., Rau, M.J, Vlachos, P.P. & Garimella, S.V., Axisymmetric wall jet development in confined jet impingement. *Phys. Fluids*, **29**, 2017, 025102.

[8] Hussein, H. J., Capp, S.P. & George, W.K., Velocity measurements in a high-Reynolds-number, momentum-conserving, axisymmetric, turbulent jet. *J. Fluid Mech.*, **258**, 1994, 31-75.

[9] Koepf, E., Villasmil, W. & Meier, A., High Temperature Flow Visualization and Aerodynamic Window Protection of a 100-kW th Solar Thermochemical Receiver-reactor for ZnO Dissociation. *Energy Procedia*, **69**, 2015, 1780-1789.

[10] Lim, J. H., Nathan, G.J., Hu, E. & Bassam, B.B., Analytical assessment of a novel hybrid solar tubular receiver and combustor. *Appl. Energy*, **162**, 2016, 298-307.

[11] Long, S., Lau, C.W.T., Chinnici, A., Tian, Z.F., Bassam, B.B. & Nathan, G.J., Experimental and numerical investigation of the iso-thermal flow characteristics within a cylindrical chamber with multiple planar-symmetric impinging jets. *Phys. Fluids*, **29**, 2017, 105111.

[12] Long, S., Lau, C.W.T., Chinnici, A., Tian, Z.F., Bassam, B.B. & Nathan, G.J., Iso-thermal flow characteristics of rotationally symmetric jets generating a swirl within a cylindrical chamber. *Phys. Fluids*, **30**, 2018, 055110.

[13] Nathan, G.J., Battye, D.L. & Ashman, P.J., Economic evaluation of a novel fuel-saver hybrid combining a solar receiver with a combustor for a solar power tower. *Appl. Energy*, **113**, 2014, 1235-1243.

[14] Nikuradse, J., Gesetzmäßigkeiten der turbulenten Strömung in glatten Rohren. *Forsch. Geb. Ingenieurwes.*, **4**, 1933, 44-44.

[15] Tanaka, E. , The interference of two-dimensional parallel jets: 1st report, experiments on dual jet. *Bull. JSME*, **13**, 1970, 272-280.

[16] Tanaka, E. , The interference of two-dimensional parallel jets: 2nd report, experiments on the combined flow of dual jet. *Bull. JSME*, **17**, 1974, 920-927.

[17] Tanaka, E. & Nakata, S., The Interference of Two-Dimensional Parallel Jets: 3rd Report, The Region near the Nozzles in Triple Jets. *Bull. JSME*, **18**, 1975, 1134-1141.

[18] Wünning, J.A. & Wünning, J.G., Flameless oxidation to reduce thermal NO-formation. *Prog. Energy Combust. Sci.*, **23**, 1997, 81-94.